Liquids in porous media

Liquids in porous media

R Lenormand

Institut Français du Pétrole, BP 311, 92506 Rueil-Malmaison Cédex, France

Abstract. The basic mechanisms which take place during the displacement of immiscible fluids in porous media have been observed in micromodels and have been modelled. At the pore level, in drainage, the invading fluid chooses the largest throat. In imbibition, the displacement depends on the local geometry. For a large pore-to-throat ratio (aspect ratio), the main mechanism is the collapse of the invading fluid in the smallest channel, without entering the pore. For a small aspect ratio, the wetting fluid invades the pore first, and then the adjacent channels. From observations at the pore level, we have modelled the displacement on a large scale in some extreme cases by using statistical theories. The different behaviours are then displayed as domains in three phase diagrams: one for drainage and two for imbibition (large and small aspect ratios). At a high rate, when viscous forces are dominant, all the diagrams show a stable domain (described by anti-DLA) and a viscous fingering domain (DLA). In drainage, low capillary numbers lead to capillary fingering represented by invasion percolation. In imbibition, the capillary domain is described either by a compact cluster growth (small aspect ratio) or percolation theory (large aspect ratio). In addition the possibility of flow by film along the roughness of the walls leads to disconnected structures.

1. Introduction

We are interested in the distribution of two immiscible fluids inside a porous medium, in order to predict transport properties. In this domain, the lack of detailed information on the mechanisms generally leads to the use of empirical parameters. By using transparent porous media, we have obtained significant insight into the physical mechanisms and we have been able to develop consistent models based on microscopic observations.

We have studied the pattern formed by a fluid (2) pushing an immiscible fluid (1), with slow displacements (no inertial effects), without any gravity effect. The pore size is large (larger than one micron) and we assume that all the interactions between the fluids and the solid can be represented by a contact angle. All the physics is then controlled by two kinds of mechanisms: viscous pressure drop and capillarity. The relative intensity of these two kinds of forces is quantified by the capillary number, defined as the ratio of viscous to capillary forces at the pore scale:

$$Ca = V_2\mu_2/\gamma \tag{1}$$

where V is a mean velocity of one fluid, μ its viscosity and γ the interfacial tension.

Another parameter is the viscosity ratio, defined by

$$M = \mu_2/\mu_1. \tag{2}$$

The contact angle is near zero and is not a parameter in the study. However, we must distinguish whether the displacing fluid is the wetting fluid (*imbibition*) or the non-wetting fluid (*drainage*).

This paper is essentially a survey of several former publications where more details can be found. However, the series of imbibition experiments and the phase diagrams for imbibition are original.

The first part of this paper gives some examples of displacements in micromodels. The second part depicts the observations of the displacement of the meniscus at the pore scale. Then, the large-scale patterns are explained and modelled for drainage and imbibition. The different types of displacement are considered in the form of phase diagrams for drainage and imbibition.
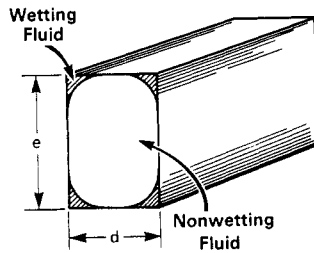

Figure 1. Situation of the fluids in a channel of the micromodel.

2. Experiments

The micromodels used in the experiments are made of transparent resin cast in a photographically etched mold [1]. We will call the cylindrical capillaries *channels*, and we will call the volumes of the intersections of the etched network *pores*. The cross section of each channel is rectangular (figure 1) with a constant depth ($e = 1$ mm) and a width d that varies from pore to pore with a given distribution and a random location. Various sizes of networks are used for the experiments with the largest one containing more than 250 000 channels. Figure 2 shows some situations of fluids in the pores after a displacement: (*a*) air and oil (gray) after drainage (air injection), (*b*) after imbibition; (*c*) mercury (black) and mercury vapor after imbibition (withdrawal).

Now we give some examples of fluid injection at a large scale, in a 40 000 channel network (130×150 mm). Each series of experiments is performed with the same fluids (same viscosity ratio M) at various flow rate (or Ca). In drainage, the non-wetting fluid is injected on the left. In imbibition, the wetting fluid is injected at the centre. In this case, the capillary number is calculated for radial injection at a distance of 30 mm from the centre.

(i) Stable drainage (figure 3): mercury displacing air ($M = 80$).

(ii) Unstable drainage (figure 4): air displacing oil ($M = 2 \times 10^{-5}$).

(iii) Stable imbibition in a square network with a narrow distribution of channel width (figure 5(*a*)): oil displacing air ($M = 2.9$); same imbibition in a triangular
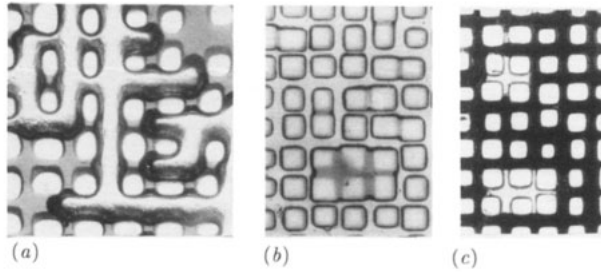
Figure 2. Close-up of various of displacements in micromodels: (*a*) drainage, air displacing oil (gray); (*b*)imbibition at very low rate (oil-air); (*c*) mercury withdrawal (liquid mercury in black).
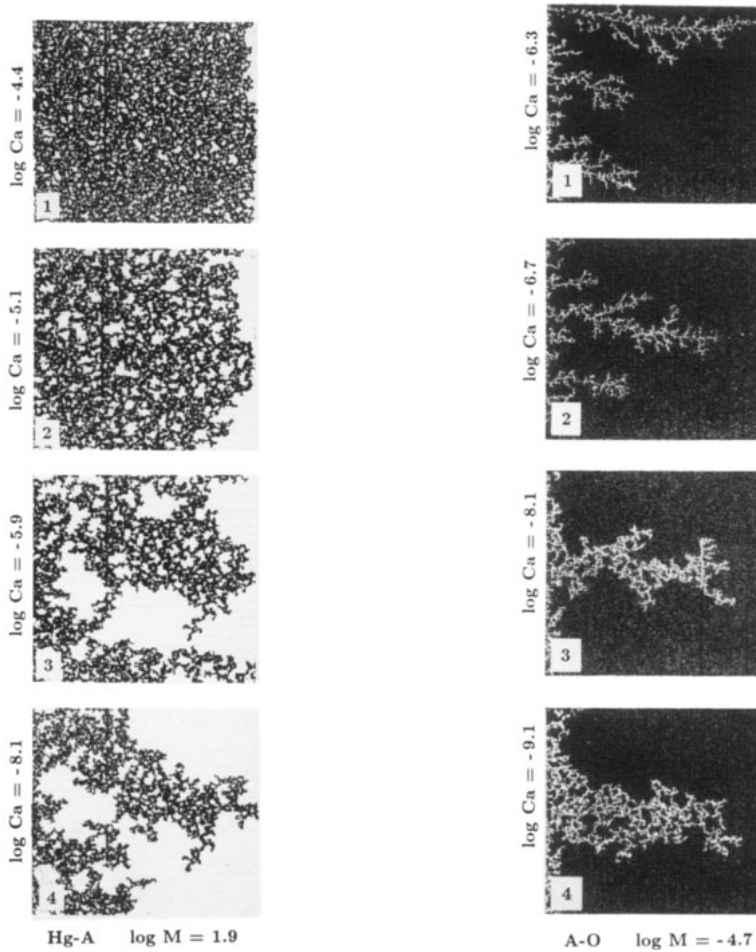
Figure 3. Drainage: injection of mercury (black) displacing air at various capillary numbers.

Figure 4. Drainage: injection of air displacing oil (black) at various capillary numbers.

network (figure 5(*b*)); same imbibition in a square network with a wide distribution of channel width (from 0.16 to 0.64 mm): figure 5(*c*).

All these experiments are examples of displacements we want to interpret. For this purpose, we will first study the mechanisms at the pore level.
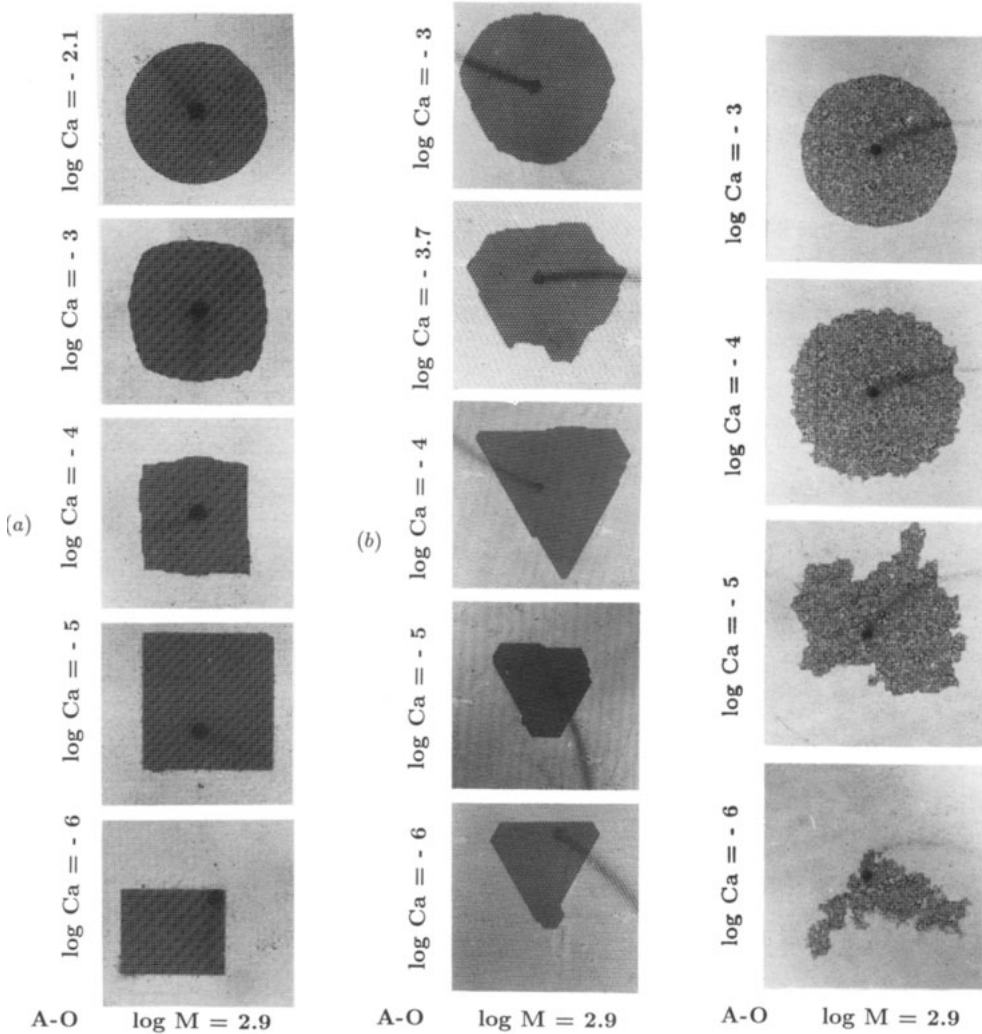
Figure 5. Imbibition. (*a*) Injection of oil (black) displacing air in a square network with a narrow pore size distribution. (*b*) Injection of oil (black) displacing air in a triangular network with a narrow pore size distribution. (*c*) Injection of oil (black) displacing air in a square network with a wide pore size distribution.

3. Physical mechanisms at the pore level

Experiments show that both fluids can flow simultaneously in the same channel with different velocities, the wetting fluid remaining in the extreme corners of the cross section and roughness of the walls (figure 1). This effect explains the richness of mechanisms involved during displacements.

A displacement can be divided into three parts: (i) flow of the injected fluid from the entrance towards the moving meniscus, (ii) displacement of the meniscus, and (iii) flow of the displaced fluid towards the exit.

3.1. Meniscus displacements

The mechanisms are different in drainage and imbibition.

In drainage, the non-wetting fluid is stopped by the throat at the entrance of a channel until the pressure exceeds the pressure in the wetting fluid by a value equal to the capillary pressure. After passsing this throat, the non-wetting fluid spontaneously invades the adjacent pore (intersection), which is larger than the channel.

In imbition, there are two additional effects due to pore geometry and also to the flow by film along the roughness of the solid. The effect of geometry, which can introduce a selection of imbibition mechanisms, have been dealt with in detail in a previous paper [2]. Similar results have also been observed in micromodels by Wardlaw and Li [3].

We found two main mechanisms.

(i) Pore invasion (figure 6). During invasion of the wetting fluid, the capillary pressure decreases and consequently the radius of curvature of the meniscus increases (figurs 6(a) and (b). At a given pressure P_1 (figure 6c), the meniscus touches the wall and instantaneously the wetting fluid invades the pore and the adjacent channels. This displacement shows some analogy with a contact line moving on a two-dimensional rough surface [4,5].

(ii) Collapse in a channel (figure 7). The wetting fluid can flow along the roughness of the walls and surround the solid grains (figure 7(a)). At a given pressure P_2, the fluid which accumulates on the walls of a channel becomes unstable and fills the channel (7(b)). This mechanism has been described under the name of *pinch-off* by Vizika and Payatakes [6].
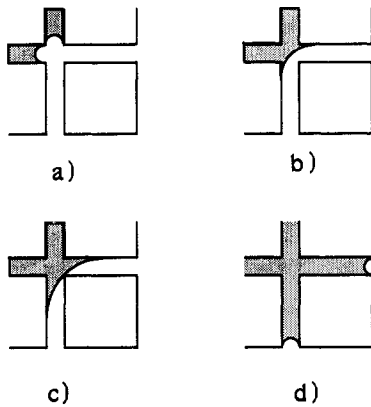

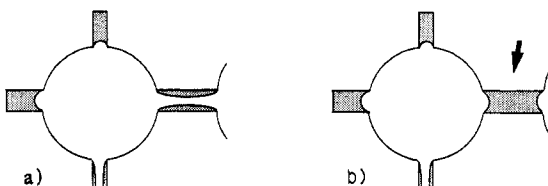**Figure 6.** Mechanism of pore invasion.

Figure 7. Mechanism of fluid collapse in a channel.

Now, in a micromodel the capillary pressure decreases when the fluid is injected. Consequently the dominant mechanism corresponds to the highest threshold pressure

(it occurs first). These pressures P_1 and P_2 can be calculated as functions of the local geometry and also of the contact angle [2]. Generally, because of the pore size distribution, both mechanisms occur during imbibition. However, we can distinguish two extreme cases, depending on the pore-to-throat ratio (aspect ratio).

(i) Small aspect ratio. When the size of the pore is small compared with channel diameters, the meniscus touches the wall very quickly (figure 6(c)) and P_1 is higher than P_2. Imbibition takes place by a succession of pore invasion. This leads to filling of the network line by line as shown in figure 8.

(ii) Large aspect ratio. In the opposite case, P_2 is greater than P_1 and the collapse inside a channel is the dominant mechanism (figure 7).

These two mechanisms lead to different patterns at a large scale: flat interfaces for a small aspect ratio and ramified structures for a large aspect ratio.
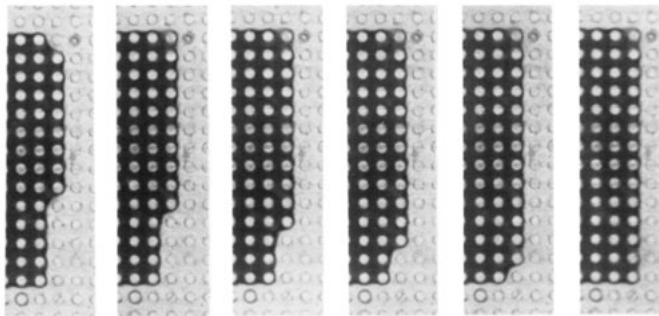

Figure 8. Different stages of the growth of a compact cluster by pore invasion.

3.2. Flow of fluids

The non-wetting (NW) fluid can flow only in the bulk of the channels. So flow occurs only if a continuous path of channels or pores filled with this phase exists towards either the entrance (during drainage) or the exit (during imbibition) of the network. Otherwise the NW fluid is trapped.

The flow of the wetting fluid is more complicated. We observe three kinds of flow of the wetting fluid: (i) flow in the bulk of the channels, (ii) along the corners when the NW fluid fills the central part of the channel and (iii) by *film* along the roughness of the walls, but only for strong wettability and very low flow rate.

4. Drainage

Now we observe the patterns formed by the injected fluid during invasion at the scale of the network.

In drainage, we have identified three main regimes for the displacement of a wetting fluid by a NW fluid. This approach leads to an original display of the corresponding domains on a general diagram with axes representing the capillary number and the viscosity ratio (figure 9). These three regimes correspond to the limits when two of the three kinds of forces involved during displacement are negligible: (i) capillary fingering, when the injection rate is very low and viscous forces are negligible in both fluids; (ii) stable displacement, at high rate when capillarity forces are low and with negligible
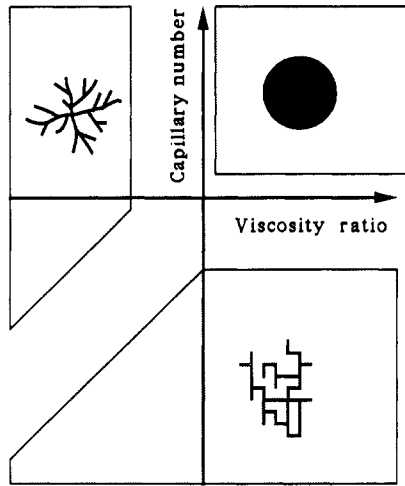
DRAINAGE

Figure 9. Phase-diagram for drainage.

pressure drop in the displaced phase (small M); and (iii) unstable displacement, in the opposite case, when the pressure drop is negligible in the injected fluid (large M).

In addition we have shown [7] that these three limit regimes can be represented by statistical models.

(i) Invasion percolation for capillary fingering [8,9]. The capillary threshold across the meniscus allows only a fraction of channels (or bonds) to be open to the flow. A computer simulation of invasion percolation is based on the following rules: a random number (between 0 and 1) is given at each bond of the network, and this number is kept fixed during the entire simulation. At each step, the interface is moved to invade the bond adjacent to the interface with the largest number.

(ii) Diffusion limited aggregation (DLA) for viscous fingering [10]. This mechanism is linked to a growing interface in a Laplacian field, which is the case for the pressure field during displacement in porous media. DLA can be represented by the following process [11]: a seed particle or a line is placed on a lattice. Another particle is lauched from a faraway source and moves at random. It is trapped when it reaches the seed or the line. Another particle is then launched, and so on. This diffusive process produces very ramified clusters similar to the injection pattern shown in figure 4-1.

(iii) Anti-DLA for stable displacement. This model is the reverse of DLA. It consists in releasing antiparticles near a compact aggregate. The antiparticle moves at random and, when it reaches a particle, both are removed.

Now, the two series of drainage experiments (figures 3 and 4) can be understood through this phase diagram. They represent the evolution with the capillary number when the viscosity ratio is kept constant: figure 3 at $M = 80$ from a stable displacement in the anti-DLA domain (1) toward capillary fingering in the percolation domain (4); figure 4 at $M = 2 \times 10^{-5}$ from an unstable displacement in the DLA domain (1) toward capillary fingering in the percolation domain (4).

In drainage, this phase diagram has been validated by a large number of experiments together with numerical simulation for a network of capillaries [7].

We will now examine the case of imbibition, which is much more complicated because of the effect of the geometry of the solid and the flow by film at a very low flow rate.

5. Imbibition

First of all, we assume that all the viscous domains are the same as for drainage. Experimentally we have verified only the stable case (figure 5) at the highest rates. In the unstable case, it seems that an important effect is the increase of the contact angle with velocity. At high rate, the injected fluid invades the central part of the channels as in drainage.

When capillary forces are great, we must account for the geometry of the solid. We will examine the two extreme cases observed at the microscopic scale and related to the ratio of pore-to-throat size (aspect ratio).

5.1. Large aspect ratio

The injected wetting fluid invades the network by a succession of collapses in the channels. Due to pressure effects, the smallest channel is filled first. Without flow by film, the filled channel is adjacent to the interface. With flow by film, this channel can be anywhere in the network. Consequently, we are filling bonds at random locations in the network, and this mechanism is related to a *bond percolation* problem. However, the topology is not the same as in drainage. As shown in figure 7(b), the collapse of the wetting fluid in the channel links the two centres of the grains. The centres of these grains form the *dual network*.

To summarize, at intermediate flow rate ($Ca \approx 10-5$ [2]), we should observe capillary fingering described by invasion percolation. At a lower rate ($Ca < 10^{-7}$, [2]), we expect ordinary percolation.
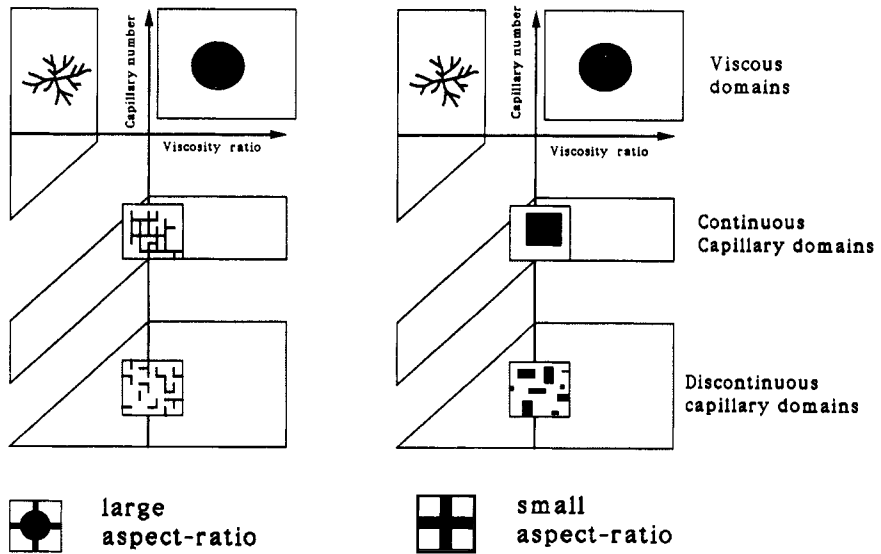
5.2. Small aspect ratio

In this case, the filling of the network line by line (figure 8) leads to a kind of *faceted crystal* growing at the injection point. The compact shape of the crystal is related to the network mesh: rectangular (figure 5(a), $\log Ca = -6$) or triangular (figure 5(b)).

For flow by film, the same mechanism occurs anywhere in the network, without any apparent connectivity with the injection. The result is an ensemble of compact clusters. We have studied the statistics of this process and have shown that, for an infinite network, there is no threshold in pressure, as opposed to percolation [12]. Figures 2(b) and 2(c) are examples of such disconnected clusters in a square network with oil (2b) and mercury (2c).

5.3. Phase diagram for imbibition

All the above-described mechanisms can be displayed in the two diagrams in figure 10(a) for a large aspect ratio and 10(b) for a small aspect ratio. In both cases, we have the *unstable and stable viscous* cases at high capillary number, an intermediate

Imbibition

Figure 10. Phase diagrams for imbibition: left-hand figure, large aspect ratio; right-hand figure, small aspect ratio.

zone for the *continuous capillary domain* (without flow by film), and at very low Ca, the *discontinuous capillary domain* (with flow by film).

In fact, these two diagrams are extreme (and theoretical) cases. In experiments in micromodels with a wide channel width distribution the clusters are more compact than in standard percolation. In fact, the geometry is intermediate between a large and a small aspect ratio.

Let us return to the series of experiments. Figures 5(a) and (b) are two cases of a small aspect ratio. The narrow distribution prevents any overlap of the mechanisms. These series start from a faceted crystal (respectively rectangular and triangular), without flow by film at low Ca. Increasing the injection rate progressively leads to stable circular displacements. Fig 5(c) is intermediate between a large and small aspect ratio, with a branched cluster close to percolation in the continuous capillary domain. Increasing the flow rate leads to a stable circular displacement.

We have no experiments showing the transition between unstable flow and faceted crystals. However, displacements of viscous oil by water have been performed by Stokes *et al* [15] in glass bead packs, which behave like small aspect ratio media. The main result is an increase in the width of the fingers when Ca decreases. In other domains of physics, similar cross-overs from ramified to compact patterns have been experimentally obtained by Skjeltorp for aggregation of uniformly sized microspheres [13] and have been simulated by Schwartz Sørensen *et al* [14] for solidification.

For imbibition, we cannot rely on numerical simulations to improve and validate these diagrams. Except cellular automata on a very small scale (a few pores [16]), there are no simulators taking into account both imbibition mechanisms and viscous effects. Cieplak and Robbins [17] simulated imbibition with various contact angles. They have taken into account the meniscus displacement, but not the flow by film (leading to the collapse mechanism) and viscous effects. Payatakes [18] improved a

simulator (with viscous effects) to represent the flow by film, but mechanisms at the pore level seem closer to drainage than imbibition.

6. Conclusion

With the help of visualizations in transparent micromodels, we have been able to describe and to model the mechanisms that take place during the displacement of immiscible fluids in porous media.

At the pore level we have observed the displacement of the meniscus. In drainage the invading fluid chooses the largest throat. In imbibition the displacement depends on the local geometry. For a large aspect ratio, the main mechanism is the collapse of the invading fluid in the smallest channel, without entering the pore. For a small aspect ratio, the wetting fluid invades the pore first, and then the adjacent channels.

From observations at the pore level, we have been able to model the displacement at a large scale by using statistical theories. The different domains have been displayed in three phase diagrams: one for drainage and two for imbibition (for a large and small aspect ratio).

At a high rate, when viscous forces are dominant, all the diagrams show a stable domain (described by anti-DLA) and a viscous fingering domain (DLA).

In drainage, low capillary numbers lead to capillary fingering represented by invasion percolation. In imbibition, the capillary domain can be decribed either by faceted crystals (small aspect ratio) or percolation (large aspect ratio). In addition the possibility of flow by film along the roughness of the walls leads to disconnected structures.

References

[1]   Lenormand R, Zarcone C and Sarr A 1983 *J. Fluid Mech.* **135** 637
[2]   Lenormand R and Zarcone C 1984 Paper presented at *59th Ann. Meeting. of Soc. Petr. Eng., Houston* paper 13264
[3]   Wardlaw N C and Li Y 1988 *Transport in porous media* **3** 17-34
[4]   Jansons K M 1985 *J. Fluid Mech.* **154** 1
[5]   Robbins M O and Joanny J F 1987 *Europhys. Lett.* **3** 729
[6]   Vizika O and Payatakes A C 1989 *PCH Physicochemical Hydrodyn* **11** 187-204
[7]   Lenormand R, Touboul E and Zarcone C 1988 *J. Fluid Mech.* **189** 165-87
[8]   Lenormand R and Zarcone C 1985 *Phys. Rev. Lett.* **54** 2226-9
[9]   Wilkinson D and Willemsen J F 1983 *J. Phys. A: Math. Gen.* **16** 3365
[10] Paterson L 1984 *Phys. Rev. Lett.* **52** 1621-4
[11] Witten T A and Sander L M 1983 *Phys. Rev.* B **27** 5686-97
[12] Lenormand R and Zarcone C 1984 in *Kinetics of Aggregation and Gelation* ed F Family and D P Landau (Amsterdam: Elsevier)
[13] Skjeltorp A T 1987 *Phys. Rev. Lett.* **58** 1444-7
[14] Schartz Sørensen E, Fogedby C and Mouritsen Ole G 1988 *Phys. Rev. Lett.* **61** 2770-3
[15] Stokes J P, Weit D A, Gollub J P, Dougherty A, Robbins M O, Chaikin P M and Lindsay H M 1986 *Phys. Rev. Lett.* **57** 1718
[16] Cieplak M and Robbins M O 1988 *Phys. Rev. Lett.* **60** 2042-5
[17] Payatakes A 1990 *Fundamentals of Fluid Transport in Porous Media (Arles, France 1990)*
[18] Rothman D H 1989 *Discrete Kinetic Theory, Lattice-gas Dynamics, and Foundations of Hydrodynamics* ed R Monaco (Singapore: World Scientific) pp 286-99